ISSN 1052-6188, Journal of Machinery Manufacture and Reliability, 2014, Vol. 43, No. 4, pp. 270–275. © Allerton Press, Inc., 2014.
Original Russian Text © O.B. Balakshin, B.G. Kukharenko, D. Peitsch, 2014, published in Problemy Mashinostroeniya i Nadezhnosti Mashin, 2014, No. 4, pp. 21–27.

MECHANICS OF MACHINES

Nonlinear Acoustic Diametral Modes of Pressure Pulsations during Flutter of Rotor Blades of a Turbocompressor

O. B. Balakshin[a], B. G. Kukharenko[a], and D. Peitsch[b]

[a] *Blagonravov Institute of Engineering Science, Russian Academy of Sciences, Moscow, Russia*
[b] *Technical University, Berlin, Germany*
e-mail: Kukharenkobg@hotmail.com

Received February 17, 2014

Abstract—Features of pressure pulsations of flow during flutter on the bending frequency of rotor blades of an axial turbocompressor, which occurs after incomplete resonance at the torsion frequency of blades with a harmonic of rotor speed, are investigated. The frequency spectrum of nonlinear acoustic diametral modes is predicted, based on Navier–Stokes equations ensemble-averaged. This makes it possible to identify characteristic series determined by the bending frequency of flutter and its second harmonic in the frequency spectrum for recording the pressure pulsation of flow during flutter along with harmonics of rotor speed. The occurrence the second harmonic of the bending frequency is the nonlinear reaction of flow, which locally limits the flutter amplitude in time.

DOI: 10.3103/S1052618814040013

The feature of the occurrence and development of classic flutter for rotor stage blades of the blisk (bladed disk) type for an axial turbocompressor in aircraft engines is that flutter at the natural frequency of blades is preceded with the resonance on the other natural frequency of the blades, which is caused by the torsion frequency harmonic of the rotor. With increasing the rotor speed, the resonance development interrupts as a result of the occurrence of flutter—synchronous vibrations of blades at their natural frequency, which is not connected by any numerical relationships with the rotor speed. The synchronization of vibrations of rotor blades in the aeroelastic system occurs because of the elasticity of the compressed air flow, in which acoustic diametral modes of pressure pulsations appear during flutter. The flutter of turbocompressor rotor blades is described by the model of circular modes of synchronous vibrations:

$$\mathbf{u}_i(t) = \sum_{m=-N_b+1}^{N_b-1} \mathbf{U}_m \exp(j(2\pi f_B t + (i-1)\sigma_m)), \quad (1)$$

in which blades of the rotor stage vibrate with natural frequency f_B of blades and constant phase shift

$$\sigma_m = \frac{2\pi m}{N_b}, \quad m = 0, \pm 1, \pm 2, ..., \pm(N_b - 1), \quad (2)$$

where N_b is the number of blades in the rotor stage of the turbocompressor. The precedence of resonance to flutter, however, with the competition of resonance and flutter for only one vibration mode of rotor blades, is established in [1].

The dependence of rotor speed f_R on the time to occurrence of the bending flutter of blades of the first stage at $f_R \approx 60$ Hz during the test of the blisk type rotor of the turbocompressor considered is represented in Fig. 1. It is established [2] that torsion modes of blades with frequency $f_T \approx 178$ Hz, which is close to harmonic $3f_R$ of the rotor speed, are primarily excited in the time interval $t = 4, \ldots, 20$ s. With increasing rotor speed, the resonance departure at frequency f_T of the torsion mode of blades occurs, and in time interval $t = 17.4, ..., 24.6$ s flutter with a positive damping factor (logarithmic decrement with the opposite sign) occurs at a lower bending frequency of the blades,

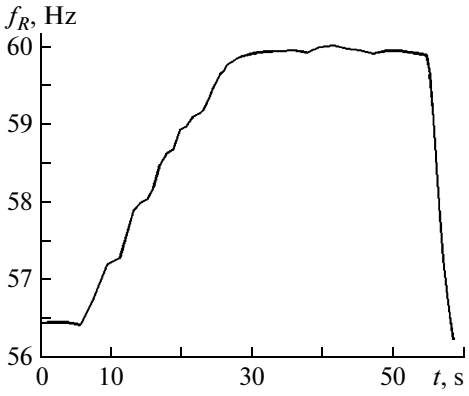

Fig. 1.

$f_B \approx 81$ Hz. The nonlinear model with antisymmetrical elastic force $F(-x) = -F(x)$ predicts bending vibrations of blades, $x = x(t)$ with the spectrum containing only odd harmonics of natural frequency f_B [3].

The linear reaction of the flow on the flutter of rotor blades is acoustic diametral modes of flow pressure pulsations [4]. In the rotor reference system they present single-frequency pulsations with the frequency of synchronous bending vibrations of blades, $f_B \approx 81$ Hz. The nonlinear flow reaction is described by Reynolds-averaged Navier–Stokes equations for the field of flow rates [5]. The Reynolds averaging over an ensemble for air flow in the axial turbocompressor for Navier–Stokes equations is obtained by averaging the instantaneous scalar and vector fields of flow for instants of time which differ by sequential periods of the rotor revolution [6]. The ensemble averaging gives the deterministic (coherent) unsteady-state density of flow

$$\langle \rho(z, r, \varphi, t)\rangle = \lim_{M\to\infty}\frac{1}{M}\sum_{m=1}^{M}\rho(z, r, \varphi, t + T_R(m-1)),$$

where $\{z, r, \varphi\}$ are cylindrical coordinates; T_R is the period of rotor revolution; and $t = [0, kT_R]$, where k is the integer.

Components $\upsilon_\alpha(z, r, \varphi, t)$, $\alpha = \{z, r, \varphi\}$ of the instantaneous field of flow rates are determined by the ensemble averaging weighted by the density (Favre averaging)

$$\begin{gathered}\langle \upsilon_\alpha(z, r, \varphi, t)\rangle \\ = \left(\lim_{M\to\infty}\frac{1}{M}\sum_{m=1}^{M}\rho(z, r, \varphi, t + T_R(m-1))\,\upsilon_\alpha(z, r, \varphi, t + T_R(m-1))\right)/\langle \rho(z, r, \varphi, t)\rangle, \\ \alpha = \{z, r, \varphi\},\end{gathered} \tag{3}$$

where $t = [0, kT_R]$, where k is the integer.

The instantaneous field of flow rates is decomposed in the deterministic (coherent) (3) and stochastic (fluctuating) field of rates

$$\upsilon_\alpha(z, r, \varphi, t) = \langle \upsilon_\alpha(z, r, \varphi, t)\rangle + \xi_\alpha(z, r, \varphi, t), \quad \alpha = \{z, r, \varphi\}, \tag{4}$$

where from (3) follows $\langle \xi_\alpha(z, r, \varphi, t)\rangle = 0$ and $\alpha = \{z, r, \varphi\}$.

The ensemble averaging of Reynolds for Navier–Stokes equations is represented in [6, 7]. The nonlinear equation for the axial moment has the form

$$\begin{gathered}\frac{\partial\langle\rho\rangle\langle\upsilon_z\rangle}{\partial t} + \frac{\partial(\langle\rho\rangle\langle\upsilon_z\rangle\langle\upsilon_z\rangle + \langle p\rangle)}{\partial z} + \frac{1}{r}\frac{\partial r\langle\rho\rangle\langle\upsilon_r\rangle\langle\upsilon_z\rangle}{\partial r} + \frac{1}{r}\frac{\partial\langle\rho\rangle\langle\upsilon_\varphi\rangle\langle\upsilon_z\rangle}{\partial\varphi} \\ = \frac{\partial(\langle\tau_{zz}\rangle - \langle\rho\xi_z\xi_z\rangle)}{\partial z} + \frac{1}{r}\frac{\partial r(\langle\tau_{rz}\rangle - \langle\rho\xi_r\xi_z\rangle)}{\partial r} + \frac{1}{r}\frac{\partial(\langle\tau_{\varphi z}\rangle - \langle\rho\xi_\varphi\xi_z\rangle)}{\partial\varphi}.\end{gathered} \tag{5}$$

Additive terms in (5) in comparison with Navier–Stokes equations are Reynolds stresses $R_{\alpha\beta} = \langle\rho\xi_\alpha\xi_\beta\rangle$, and $\alpha, \beta = \{z, r, \varphi\}$ in the form of correlation of stochastic fields from (4).

Equation (5) describes the nonlinear reaction of the field of flow rates on the vibration of surfaces of rotor blades on its boundaries. In the case of the single-frequency vibration of blades, $x_b = A_x\sin(2\pi f_B t)$, the time dependence of deterministic (coherent) components $\langle\upsilon_z\rangle$ and $\langle\upsilon_\varphi\rangle$ of the flow rate field is represented by Fourier series

$$\begin{aligned}\langle\upsilon_z\rangle &\propto A_1\sin(2\pi f_B t + \theta_{z1}) + A_2\sin(4\pi f_B t + \theta_{z2}) + \ldots, \\ \langle\upsilon_\varphi\rangle &\propto B_1\sin(2\pi f_B t + \theta_{\varphi 1}) + B_2\sin(4\pi f_B t + \theta_{\varphi 2}) + \ldots\end{aligned} \tag{6}$$

In (6) the terms with the first harmonic describe the ensemble-averaged (3) linear reaction of flow,

$$\langle\upsilon_z\rangle \propto A_1\sin(2\pi f_B t + \theta_{z1}), \quad \langle\upsilon_\varphi\rangle \propto B_1\sin(2\pi f_B t + \theta_{\varphi 1})$$

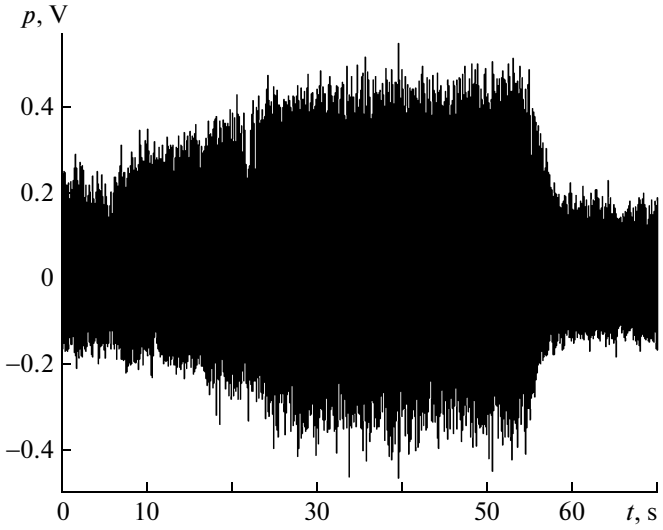

Fig. 2.

with bending frequency f_B of blade vibrations. By the method of harmonic balance, terms with the second harmonic of the bending frequency in (6) are considered as disturbances in (5) by nonlinear terms $\langle\rho\rangle\langle\upsilon_\alpha\rangle\langle\upsilon_\beta\rangle$, $\alpha, \beta = \{z, r, \varphi\}$ in the form

$$\begin{aligned}\langle \upsilon_z\rangle\langle \upsilon_\varphi\rangle &\propto A_1\sin(2\pi f_B t + \theta_{z1})B_1\sin(2\pi f_B t + \theta_{\varphi 1}) + \ldots \\ &= \frac{A_1B_1}{2}(\cos(\theta_{z1} - \theta_{\varphi 1}) - \cos(4\pi f_B t + \theta_{z1} + \theta_{\varphi 1})) + \ldots.\end{aligned} \tag{7}$$

The average value $\langle\rho(\upsilon_z - \langle\upsilon_z\rangle)(\upsilon_\varphi - \langle\upsilon_\varphi\rangle)\rangle$ for $M = 100$–1000 sequential instantaneous fields of flow rates is used in experimental investigations of flow in axial turbocompressors as the evaluation of Reynolds stresses in (5) [10]. This evaluation also contains the contribution of the coherent field of flow rates (3).

The record of pulsations of flow pressure $p = p(t)$ in the first stage stator of the axial turbocompressor considered with increasing rotor speed to $f_R \approx 60$ Hz is given in Fig. 2 (sampling frequency ≈20 kHz during recording). In the coordinate system connected with the rotor, every circular mode of synchronous vibrations of blades (1) with number m of nodal diameters (2) corresponds to the circular mode of flow pressure pulsations with the same number m of nodal diameters, which is called as the acoustic diametral mode of order m. Let φ be the angle along the rotor stage circumference. In the coordinate system connected with the rotor, the formula similar to (1) for the ensemble-averaged distribution of the air flow pressure subject to second harmonic f_B has the form

$$\langle p^R(t, \varphi)\rangle = \sum_{m=-N_b+1}^{N_b-1} p_m^{(0)}(\exp(j2\pi f_B t) + p_m^{(1)}\exp(j4\pi f_B t))\exp(jm\varphi). \tag{8}$$

Transition into the reference frame connected with the stator of the axial turbocompressor (with fixed guide blades) corresponds to transform $\varphi \longrightarrow \varphi + 2\pi f_R t$ (f_R is the rotor speed). Formula (8) takes the form

$$\begin{aligned}\langle p^F(t, \varphi)\rangle &= \sum_{m=-N_b+1}^{N_b-1} p_m^{(0)}(\exp(j2\pi f_B t) + p_m^{(1)}\exp(j4\pi f_B t))\exp(jm(\varphi + 2\pi f_R t)) \\ &= \sum_{m=-N_b+1}^{N_b-1} (p_m^{(0)}\exp(j2\pi(f_B + mf_R)t) + p_m^{(1)}\exp(j2\pi(2f_B + mf_R)t))\exp(jm\varphi).\end{aligned} \tag{9}$$

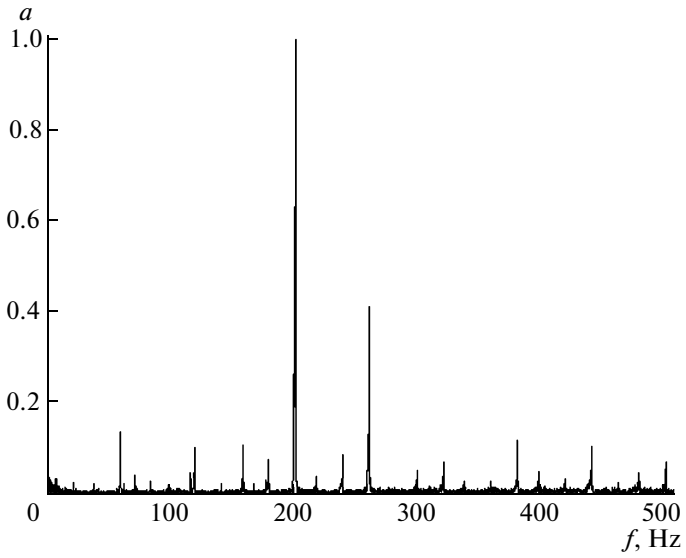

Fig. 3.

From (9) follows that lowest frequencies $f_{mD}^{(0)}$ and $f_{mD}^{(1)}$ of the acoustic mode with m nodal diameters for pressure pulsations of air flow are determined by formulas

$$f_{mD}^{(0)} = f_B + mf_R \ , \tag{10}$$

$$f_{mD}^{(1)} = 2f_B + mf_R \ . \tag{11}$$

Figure 3 shows spectral component amplitudes $a = a(f)$, determined by a fast Fourier transform, relative to the amplitude at frequency $f_{2D}^{(0)} \approx 201$ Hz of the second acoustic diametral mode for the record of flow pressure pulsations (Fig. 2). The frequency spectrum (Fig. 3) contains frequencies of acoustic diametral modes, $f_{mD}^{(0)}$, $m = 1, ..., 7$ (10) and $f_{mD}^{(1)}$, $m = 1, ...,5$ (11), and also rotor speed harmonics f_R, $m = 1, ..., 7$. In the case of transition into the reference frame connected with the stator of the axial turbocompressor, rotor speed harmonics present in flow pressure pulsations are transformed by the formula similar to (10) and (11) therefore they always are present in records of flow pressure pulsations, providing resonance at circular frequency $f_T \approx 178$ Hz which precedes the bending flutter of blades.

The time-dependent spectral parameters of the record of flow pressure pulsations (Fig. 2) are determined by the Proni method [2]. The spectral decomposition of an arbitrary segment with length N for the total record of flow pressure pulsations (time series) $p_k = p(k\Delta t)$, $k = 1, \ldots, N_0$ (below for short, it is considered that the time discretization interval $\Delta t = 1$) has the form

$$p_k = \sum_{l=1}^{M} r_l z_l^{k-1} + n_k, \quad k = 1, \ldots, N, \tag{12}$$

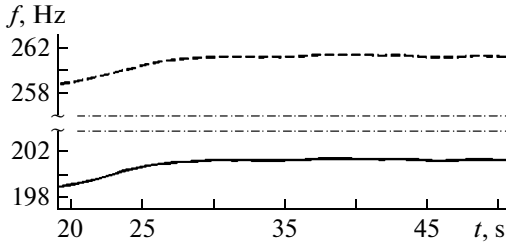

Fig. 4.

where M is the number of poles for the segment; $z_l = \exp(\delta_l + j2\pi f_l)$, $l = 1, ..., M$ are poles (δ_l and f_l are the damping factor (logarithmic decrement with the opposite sign) and the frequency, respectively); $r_l = A_l \exp(j\varphi_l)$, $l = 1, ..., M$ are pole residues (A_l and φ_l are the amplitude and the phase, respectively); and n_k is the additive noise.

The time dependence of spectra of damping factors and frequencies, $\{\delta_l, f_l, l = 1, ..., M\}$, and spectra of amplitudes and phases corresponding to them, $\{A_l, \varphi_l, l = 1, ..., M\}$, is estimated by the record in Fig. 2 as a result of sequential non-integral shifts of the time window with fixed length $N = 2000$

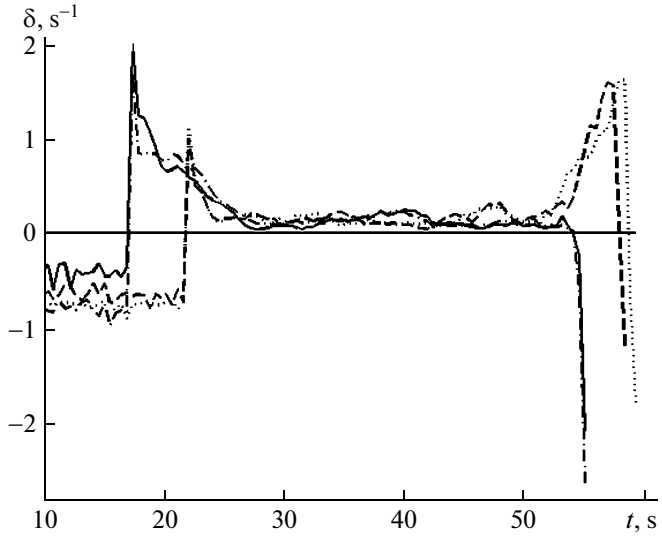

Fig. 5.

(time window size of 0.1 s). The most demonstrative evidence of nonlinearity of flow pressure pulsations in Fig. 3 is the small amplitude at frequency $f_{1D}^{(0)} \approx 141$ Hz in comparison with the amplitude at frequency $f_{1D}^{(1)} \approx 222$. However, the damping at this frequency can not be estimated because of the very large amplitude on neighboring frequency $f_{2D}^{(0)} \approx 201$ Hz.

Figure 4 shows time dependences of frequencies derived from f_B: $f_{2D}^{(0)}$ (solid line) and $f_{3D}^{(0)}$ (dashed line). They reproduce the time dependence of rotation frequency f_R (Fig. 1) by formula (10). Figure 5 shows time dependencies of the damping factor for frequencies derived from f_B (10): $f_{2D}^{(0)}$ (solid line) and $f_{3D}^{(0)}$ (chain line) and frequencies derived from the second harmonic of f_B (11): $f_{2D}^{(1)}$ (dashed line) and $f_{3D}^{(1)}$ (dotted line). The damping factor at frequencies $f_{2D}^{(1)}$ (dashed line) and $f_{3D}^{(1)}$ (dotted line) at $t = 22$ s (flutter establishment) abruptly changes its value to plus. This abrupt increase in the damping factor repeats with the flutter disappearance at $t = 55.7$ s i.e., energy in flow pressure pulsations is redistributed between frequencies derived from f_B (10) and frequencies derived from $2f_B$ (11). In Fig. 3 after $t = 58.3$ s, frequency $f_{1D}^{(1)} \approx 222$ Hz derived from harmonic $2f_B$ generally prevails in residual pulsations of flow pressure. Therefore, the presence of the second harmonic of blade bending frequency $f_B \approx 81$ Hz in the record of vibrations of blades of the first stage of the rotor investigated in [2] is caused by air flow pressure pulsations (Fig. 2).

At present, in the framework of the European Research Project FUTURE (Flutter-Free Turbomachinery Blades), the theoretical analysis of flow ensemble-averaged with respect to velocity field is carried out for the estimation of the degree of flow nonlinearity as the condition of limitation in the flutter amplitude for blades of the rotors of axial turbocompressors [11, 12].

REFERENCES

1. Ganiev, R.F., Balakshin, O.B., and Kukharenko, B.G., Resonance bifurcation under blades flatter for turbocompressor's rotor, *Dokl. Akad. Nauk*, 2012, vol. 444, no. 1, pp. 35–37.
2. Balakshin, O.B. and Kukharenko, B.G., Spectral analysis of turbocompressor's blades flatter, *Dokl. Akad. Nauk*, 2007, vol. 417, no. 5, pp. 627–630.
3. Mickens, R.E., *Truly Nonlinear Oscillations. Harmonic Balance, Parameter Expansions, Iteration, and Averaging Methods*, Singapore: World Sci., 2010.
4. Ganiev, R.F., Balakshin, O.B., and Kukharenko, B.G., Flow modes under blades flatter stabilization for turbocompressor's rotor, *Dokl. Akad. Nauk*, 2013, vol. 448, no. 6, pp. 651–653.

5. Ganiev, R.F. and Ukrainskii, L.E., *Nelineinaya volnovaya mekhanika i tekhnologii. Volnovye i kolebatel'nye yavleniya v osnove vysokikh tekhnologii* (Nonlinear Waves Mechanics and Technologies. Wave and Oscillation Phenomena as a Base of High Technology), Izhevsk: Nauch.-Izd. Tsentr "Regulyarnaya i khaoticheskaya dinamika," 2011.
6. Adamczyk, J.J., Aerodynamic analysis of multistage turbomachinery flows in support of aerodynamic design, *ASME J. Turbomachin.*, 2000, vol. 122, no. 2, pp. 189–217.
7. Simon, J.F. and Leonard, O., Modeling of 3-D losses and deviations in a throughflow analysis tool, *J. Thermal Sci.*, 2007, vol. 16, no. 3, pp. 208–214.
8. He, L. and Denton, J.D., An experiment on unsteady flow over oscillating airfoil, *Proc. ASME TURBO EXPO (IGTI)*, 1991.
9. He, L., *Unsteady Flow and Aeroelasticity*, chapter 5: *Handbood of Turbomachinery*, Logan, E. and Roy, R., Eds., New York: Marcel Dekker, 2003, pp. 268–318.
10. Chow, Y.C., Uzol, O., and Katz, J., Flow non-uniformities and turbulent "hot spots" due to wake-blade and wake-wake interactions in a multistage turbomachine, *ASME J. Turbomachin.,* 2002, vol. 124, pp. 553–563.
11. Fransson, T. and Vogt, D., FUTURE: flutter-free turbomachinery blades, *Proc. 6th European Aeronautics Days (Aerodays 2011)*, Madrid: DG Research and Innovation European Commission, 2011.
12. Freund, O., Bartelt, M., Seume, J.R., Mittelbach, M., Montgomery, M., and Vogt, D., Impact of the flow on an acoustic excitation system for aeroelastic studies, *Proc. Turbine Technical Conf. & Exposition (TURBO EXPO)* Copenhagen: ASME International Gas Turbine Institute, 2012.

Translated by S. Ordzonikidze